ZESZYTY NAUKOWE POLITECHNIKI ŚLĄSKIEJ 2005
Seria: GÓRNICTWO z. 266 Nr kol. 1689

Michał JASIŃSKI, Piotr WODZIŃSKI
Technical University, Łódź

INVESTIGATION OF SELF-SYNCHRONISATION OF VIBRATORS IN A LINEAR-ELLIPTIC SCREEN[1]

Summary. A characteristic feature of circling single-plane screens is a riddle vibrating in the longitudinal plane of the machine, i.e. in the plane perpendicular to a sieve surface and parallel to side walls of the riddle, and to resultant direction of the material transport on the sieve. At present, machines of this type constitute at least 90% of all tested and operating screening machines. Designers of these machines often take advantage of the phenomenon of self-synchronisation of driving systems of the vibrators. This allows them to significantly simplify the construction of a driving system, and consequently, to reduce its failure frequency and operating costs of screens.

This study includes results of investigations carried out in a linear-elliptic screen, one of screening machines constructed in the Department of Process Equipment, Faculty of Process and Environmental Engineering, Łódź Technical University.

BADANIE ZJAWISKA SAMOSYNCHRONIZACJI WIBRATORÓW W PRZESIEWACZU LINIOWO-ELIPTYCZNYM

Streszczenie. Przesiewacze krążące jednopłaszczyznowe charakteryzują się tym, że rzeszoto wykonuje ruch drgający w płaszczyźnie wzdłużnej maszyny, tzn. w płaszczyźnie prostopadłej do powierzchni sita i równoległej do ścian bocznych rzeszota, oraz do wypadkowego kierunku transportu materiału na sicie. W chwili obecnej maszyny tego typu stanowią co najmniej 90% badanych i eksploatowanych maszyn przesiewających. Coraz częściej konstruktorzy tego typu maszyn wykorzystują zjawisko samosynchronizacji wibratorów napędowych. Pozwala to w znacznym stopniu uprościć konstrukcję układu napędowego przesiewacza, a co za tym idzie - zmniejszyć jego awaryjność i koszty obsługi.

W niniejszym opracowaniu przedstawiono wyniki badań przeprowadzonych na przesiewaczu liniowo-eliptycznym, jednej z konstrukcji, które powstały w Katedrze Aparatury Procesowej Wydziału Inżynierii Procesowej i Ochrony Środowiska Politechniki Łódzkiej.

[1] The study was made within basic research program carried out in the Department of Process Equipment, Technical University of Łódź, Dz. St. 12.2.

Introduction

A characteristic feature of circling single-plane screens is a riddle vibrating in the longitudinal plane of the machine, i.e. in the plane perpendicular to a sieve surface and parallel to side walls of the riddle, and to resultant direction of the material transport on the sieve [1,2,3,4]. At present, machines of this type constitute at least 90% of all tested and operating screening machines. Designers of these machines often take advantage of the phenomenon of self-synchronisation of driving systems of the vibrators. This allows them to significantly simplify the construction of a driving system, and consequently, to reduce its failure frequency and operating costs of screens.

An experimental screen

This study includes results of investigations carried out in a linear-elliptic screen, one of screening machines constructed in the Department of Process Equipment, Faculty of Process and Environmental Engineering, Łódź Technical University [5]. This is a modern machine that enables simultaneous application of all known solutions for particular screen components, e.g. suspensions, sieves, sieve mounting, etc.

The screen consists of two driving vibrators and a rectangular riddle mounted on a spring suspension. Basic dimensions of the riddle are shown in Fig. 1. In this screen it is possible to change the riddle inclination from 0 to 20° and spacing of vibrators from 0 mm to 800 mm. The screen has a sieve of dimensions B*L=300*1300 mm and total vibrating mass 180 kg. The screen is driven by electrovibrators of rated speed n = 1400 min^{-1}. The speed is adjustable by changing the frequency of supply current. Additionally, it is possible to adjust exciting force of the vibrators by changing the mutual position of unbalanced masses. Usually, one rated rotational speed is used in the test. The driving system makes it possible to apply two different drive configurations: $\omega_1 = \omega_2$ and $\omega_1 = -\omega_2$.

In the above notation ω_1 and ω_2 denote angular velocities of particular driving vibrators, respectively. The notation $\omega_1 = \omega_2$ denotes cocurrent self-synchronisation of vibrators, i.e. the case when shafts of these vibrators rotate in the same directions. The notation $\omega_1 = -\omega_2$ represents counter-current self-synchronisation of driving vibrators, which

denotes spontaneous, synchronous movement of unbalanced shafts rotating in opposite directions.

As it was mentioned earlier, the screen has an adjustable spacing of electrovibrators relative to the centre of gravity of the riddle. Research on the linear-elliptic screen covers three different settings of the electrovibrators, i.e., when they are displaced relative to the riddle centre: the upper one in the feeder direction and the lower in the direction of the screen end at the distance of 50, 200 and 400 mm (setting 1, 2 and 3, respectively).

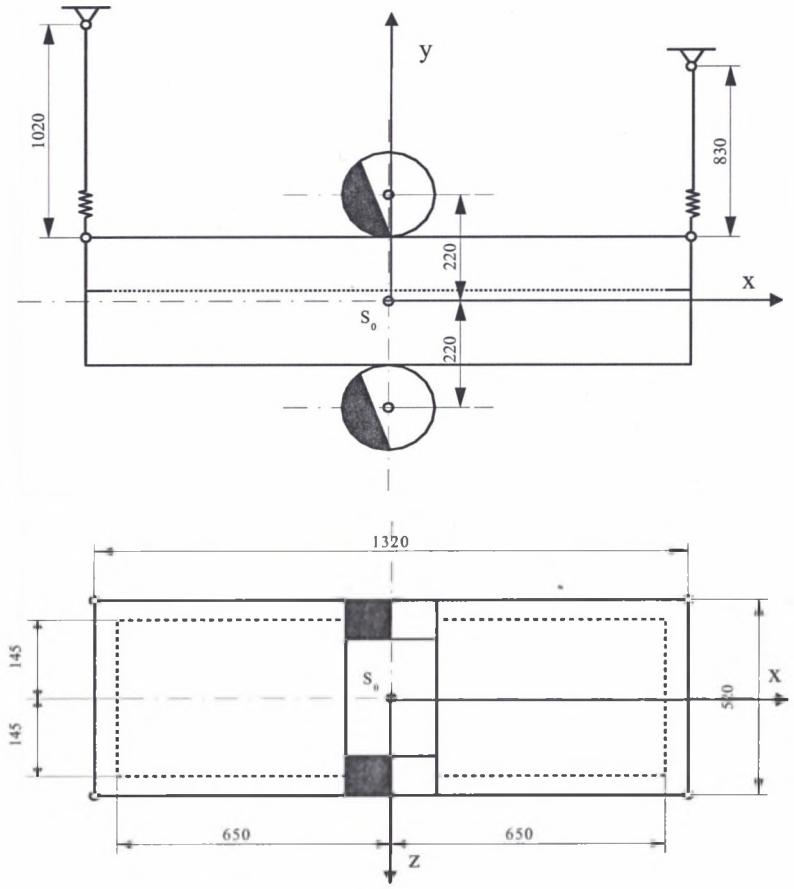

Fig. 1. Basic riddle dimensions of the linear-elliptic screen
Rys. 1. Podstawowe wymiary rzeszota przesiewacza liniowo-eliptycznego

A change in the electrovibrators spacing caused a change in the theoretical angle of sieve trajectory β (Fig. 2). In the case of the above mentioned settings of the vibrators, theoretical angles of sieve trajectories β are as follows:

$\beta_1 = 12.8^\circ$ (setting 1),

$\beta_2 = 42.3^\circ$ (setting 2),

$\beta_3 = 61.2^\circ$ (setting 3).

Additionally, a change in the setting of vibrators alters mass moment of inertia of the riddle which has a significant effect on the machine dynamics.

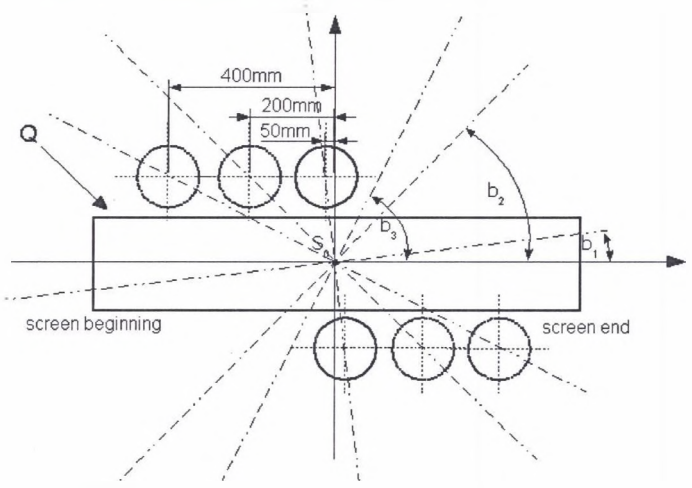

Fig. 2. Setting of electrovibrators
Rys. 2. Ustawienia elektrowibratorów

Equations of riddle motion

In the state of equilibrium of the screen body, a dextrorotatory system of coordinates x, y, z was drawn from mass centre S_o. The suspended body of the screen has 6 degrees of freedom in space. However, due to the lack of exciting forces acting in z direction, the tested system was limited to plane xy lateral to the sieve. The angles of revolution of the screen body around the transverse axis z are denoted as φ_z.

A subject studied is the motion of mass centre of the screen body of mass M and the moment of inertia relative to the transverse axis (z) denoted as I_z. The screen is suspended on four identical springs of vertical rigidity k_y and longitudinal rigidity k_x. Damping coefficients of the system along the axes are c_x and c_y, respectively.

To generate equations of motion, Lagrange's equation in the following form was used [2]:

$$\frac{d}{dt}\left(\frac{\partial L}{\partial \dot{q}_i}\right) - \frac{\partial L}{\partial q_i} + \frac{\partial P}{\partial \dot{q}} \tag{1}$$

where:

L – Lagrangian function of the system $L = T - U$;

T – kinetic energy of the system;

U – potential energy of the system;

P – function of energy dissipation.

To simplify the calculations, a system of coordinates overlapping theoretical trajectories of the riddle motion was assumed (Fig. 3).

The total kinetic energy of the system can be described by the equation:

$$T = \frac{1}{2}\cdot m_0\cdot\left(x'^2 + y'^2\right) + \frac{1}{2}\cdot I_0\cdot\phi'^2 + \frac{1}{2}\cdot m\cdot\left(x' + b\cdot\phi' + \omega_1\cdot r\cdot\cos\left(\omega_1\cdot t\right)\right)^2 + \frac{1}{2}m\left(y' - \omega_1\cdot r\cdot\sin\left(\omega_1\cdot t\right)\right)^2 \ldots$$
$$+\frac{1}{2}\cdot I\cdot\omega'_1{}^2 + \frac{1}{2}\cdot m\left(x' - b\cdot\phi' + \omega_2\cdot r\cdot\cos\left(\omega_2\cdot t\right)\right)^2 + \frac{1}{2}m\left(y' - \omega_2\cdot r\cdot\sin\left(\omega_2\cdot t\right)\right)^2 + \frac{1}{2}\cdot I\cdot\omega'_2{}^2 \tag{2}$$

The total potential energy of the systems is:

$$U = k_y\cdot\left(y - a_{x1}\cdot\phi\right)^2 + k_y\cdot\left(y - a_{x2}\cdot\phi\right)^2 + k_x\cdot\left(x - a_{y1}\cdot\phi\right)^2 + k_x\cdot\left(x - a_{y2}\cdot\phi\right)^2 \tag{3}$$

The function of energy dissipation:

$$P = \frac{1}{2}c_y\cdot\left(y' - a_{x1}\cdot\phi'\right)^2 + \frac{1}{2}c_y\cdot\left(y' - a_{x2}\cdot\phi'\right)^2 + \frac{1}{2}c_x\cdot\left(x' - a_{y1}\cdot\phi'\right)^2 + \frac{1}{2}c_x\cdot\left(x' - a_{y2}\cdot\phi'\right)^2 \tag{4}$$

Substituting subsequent independent coordinates into equation (1), the following equations of the screen motion were obtained:

$$0 = M\cdot x'' - mr\cdot\omega_1{}^2\cdot\sin\left(\omega_1\cdot t\right) - mr\cdot\omega_2{}^2\cdot\sin\left(\omega_2\cdot t\right) + 2\cdot k_x\cdot\left(x - a_{y1}\cdot\phi\right) \ldots$$
$$+2\cdot k_x\cdot\left(x - a_{y2}\cdot\phi\right) + c_x\cdot\left(x' - a_{y1}\cdot\phi'\right) + c_x\cdot\left(x' - a_{y2}\cdot\phi'\right) \tag{5}$$

$$0 = M\cdot y'' - mr\cdot\omega_1{}^2\cdot\cos\left(\omega_1\cdot t\right) - mr\cdot\omega_2{}^2\cdot\cos\left(\omega_2\cdot t\right) + 2\cdot k_y\cdot\left(y - a_{x1}\cdot\phi\right) \ldots$$
$$+2\cdot k_y\cdot\left(y - a_{x2}\cdot\phi\right) + c_y\cdot\left(y' - a_{x1}\cdot\phi'\right) + c_y\cdot\left(y' - a_{x2}\cdot\phi'\right) \tag{6}$$

$$0 = I_0 + 2\cdot m\cdot b^2\cdot\phi'' - m\cdot b\cdot\omega_1{}^2\cdot r\cdot\sin\left(\omega_1\cdot t\right) + m\cdot b\cdot\omega_2{}^2\cdot r\cdot\sin\left(\omega_2\cdot t\right) \ldots$$
$$+ -2\cdot k_y\cdot\left(y - a_{x1}\cdot\phi\right)\cdot a_{x1} - 2\cdot k_y\cdot\left(y - a_{x2}\cdot\phi\right)\cdot a_{x2} - 2\cdot k_x\cdot\left(x - a_{y1}\cdot\phi\right)\cdot a_{y1} - 2\cdot k_x\cdot\left(x - a_{y2}\cdot\phi\right)\cdot a_{y2} \ldots$$
$$+ -c_y\cdot\left(y' - a_{x1}\cdot\phi'\right)\cdot a_{x1} - c_y\cdot\left(y' - a_{x2}\cdot\phi'\right)\cdot a_{x2} - c_x\cdot\left(x' - a_{y1}\cdot\phi'\right)\cdot a_{y1} - c_x\cdot\left(x' - a_{y2}\cdot\phi'\right)\cdot a_{y2} \tag{7}$$

The equations of motion were solved numerically assuming experimental screen parameters. The most significant numerical data assumed in the calculations are given in Table 1.

Table 1

Characteristic data of the experimental screen

m = 180 kg (screen mass)
$k_y = k_x$ = 21712 N/m. (rigidity of the system in direction y and x)
$c_x = c_y$ = 3157 N·s/m
I_0 = 39.476 to 60.332 kgm^2 (mass moment of inertia relative to axis depending on the setting of vibrators)
$\omega_1 = \omega_2$= 146 rds/s (angular velocities of the vibrators)

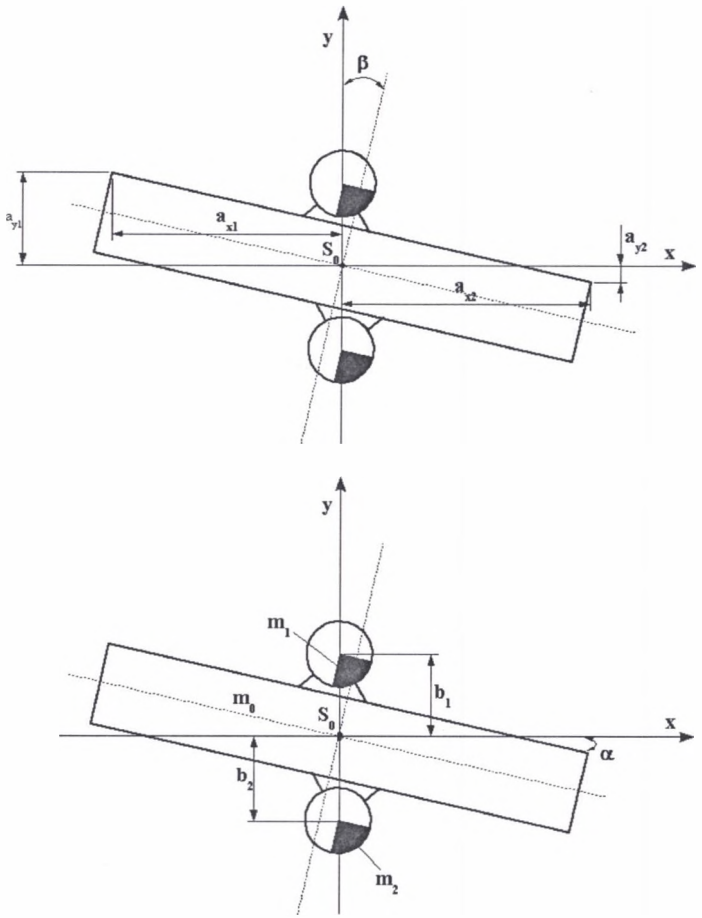

Fig. 3. Symbols used in determination of riddle motion equations
Rys. 3. Oznaczenia używane przy wyznaczaniu równań ruchu rzeszota

Since the rotational speed of the vibrators is constant (ω = 146 rad/s), in equations (5), (6) and (7) the substitutions $\omega_1 = \omega$ and $\omega_2 = \gamma \bullet \omega$ were applied.

Coefficient γ [1] determines the type of synchronisation and assumes the values:

$\gamma = 1$ for cocurrent synchronisation, and

$\gamma = -1$ for counter-current synchronisation.

Results of calculations were concordant with the real trajectories after including phase shift between the electrovibrators (Figs. 4 and 5). Phase shift λ was taken into account by inserting expression $\gamma \cdot \omega \cdot t + \lambda$ to relevant terms in equations (5) through (7). This notation [1] is generally used in the description of dynamic self-synchronisation of unbalanced vibrators (drive shafts).

The phase shift between electrovibrators has a significant effect on the character of riddle motion [1]. This effect covers transition from the circular motion to torsional vibrations of the riddle in the case of cocurrent operation of the vibrators and the change of the angle of trajectory of mass centre of the screen and character of motion of the riddle edges in the case of counter-current riddle operation (Fig. 6). These changes have a primary effect on basic process parameters of the screen, i.e. dynamic factor K and material transport velocity on the sieve surface u.

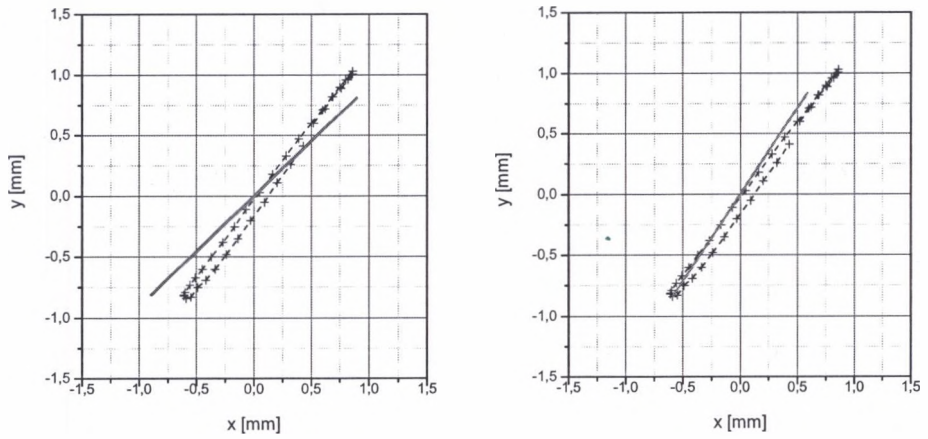

Fig. 4. Comparison of simulation results (solid line) with real riddle trajectory (broken line with points) for calculations: a) the angle of phase shift not included, b) the phase shift between the electrovibrators included (setting 1, F = 2 kN counter-current synchronisation)

Rys. 4. Porównanie wyników symulacji (linia ciągła) z rzeczywistym torem ruchu rzeszota (linia przerywana z punktami) dla obliczeń: a) nie uwzględniających kąta przesunięcia fazowego, b) uwzględniających przesunięcie fazowe między elektrowibratorami (Ustawienie 1, F = 2 kN synchronizacja przeciwbieżna)

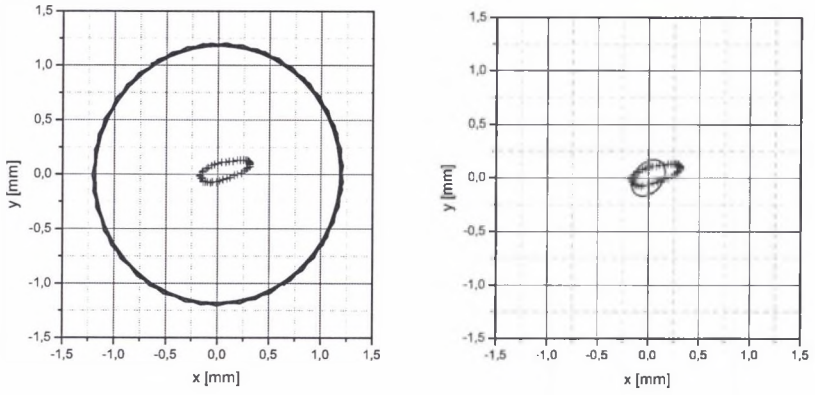

Fig. 5. Comparison of simulation results (solid line) with the real riddle trajectory (broken line with points) for calculations: a) the angle of phase shift not included, b) the phase shift between the electrovibrators included (setting 2, F = 2 kN cocurrent synchronisation)

Rys. 5. Porównanie wyników symulacji (linia ciągła) z rzeczywistym torem ruchu rzeszota (linia przerywana z punktami) dla obliczeń: a) nie uwzględniających kąta przesunięcia fazowego, b) uwzględniających przesunięcie fazowe między elektrowibratorami (Ustawienie 2, F = 2 kN synchronizacja współbieżna)

Results obtained in theoretical calculations made the authors analyse the phenomenon of self-synchronisation of vibrators in the linear-elliptic screen. For this purpose the riddle of the screen was filmed during operation and on this basis the angles of phase shift between unbalanced masses of the vibrators were determined.

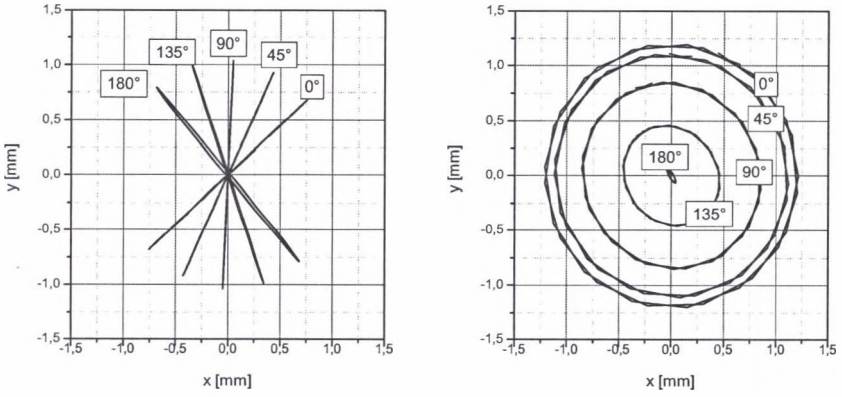

a) b)

Fig. 6. The effect of phase shift λ on the motion of mass centre of the riddle: a) counter-current synchronisation, b) cocurrent synchronisation

Rys. 6. Wpływ przesunięcia fazowego λ na ruch środka masy rzeszota przesiewacza: a) synchronizacja przeciwbieżna, b) synchronizacja współbieżna

Measuring methods

Tests were carried out using a SVHS digital camera that filmed the screen motion at the rate of 250 frames per second. The camera was set in motion after screen operation conditions stabilised, i.e. after around one minute after start. The time of filming was 2 s, which gave 500 frames on the whole. The test was repeated after 2 min of the screen operation. Next, every 20^{th} frame was subjected to computer processing to determine the angle of phase shift. Figure 7 shows a schematic diagram of the measuring set-up.

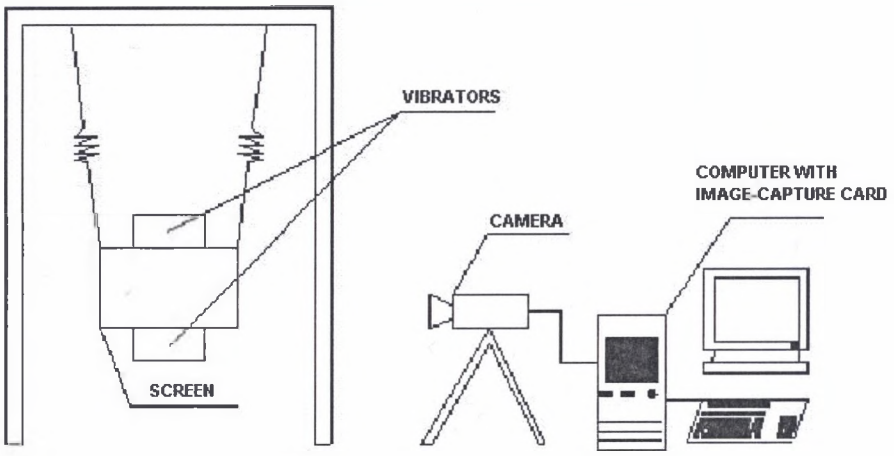

Fig. 7. Measuring system
Rys. 7. Układ pomiarowy

Measurements were carried out in the riddle suspended at the angle 15°. In the tests, the position of vibrators relative to the centre of the riddle gravity were changed (setting 1 – 50 mm, setting 2 – 200 mm, setting 3 – 400 mm, respectively, Fig. 2), and exciting force of the vibrators were changed (F = 2kN, 4.77 kN, 10 kN, respectively). Figures 7 to 9 show images obtained after processing of the recorded films.

Next, on the images obtained in this way, the angle ϕ_1 (upper vibrator) and angle ϕ_2 (lower vibrator) were measured. Figures 8 to 10 illustrate the measuring technique. The assumed procedure and the quality of photographs allowed us to determine angles ϕ with accuracy ±3°. Then, the angle of phase shift λ was calculated taking into account the geometric relations between real direction of the exciting force and tracer placed on the unbalanced mass surface. The relations for particular settings are given below:

Synchronisation $\omega_1=-\omega_2$

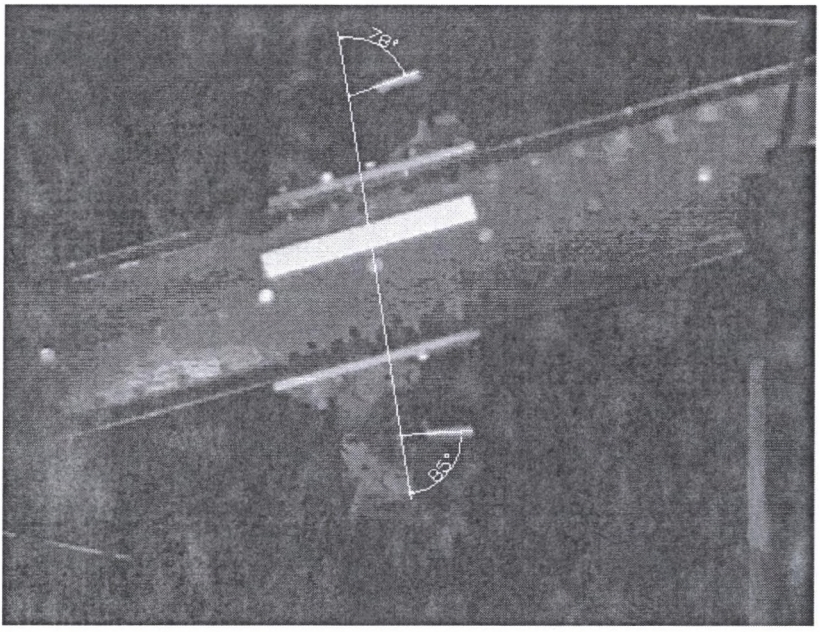

Synchronisation $\omega_1=\omega_2$

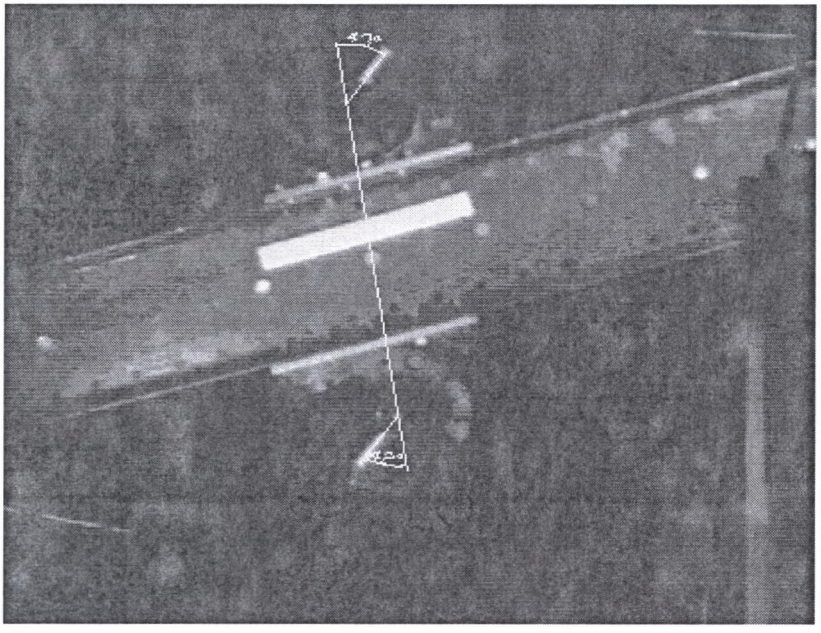

Fig. 8. Setting 1, F = 10 kN
Rys. 8. Ustawienie 1, F = 10 kN

Synchronisation $\omega_1=-\omega_2$

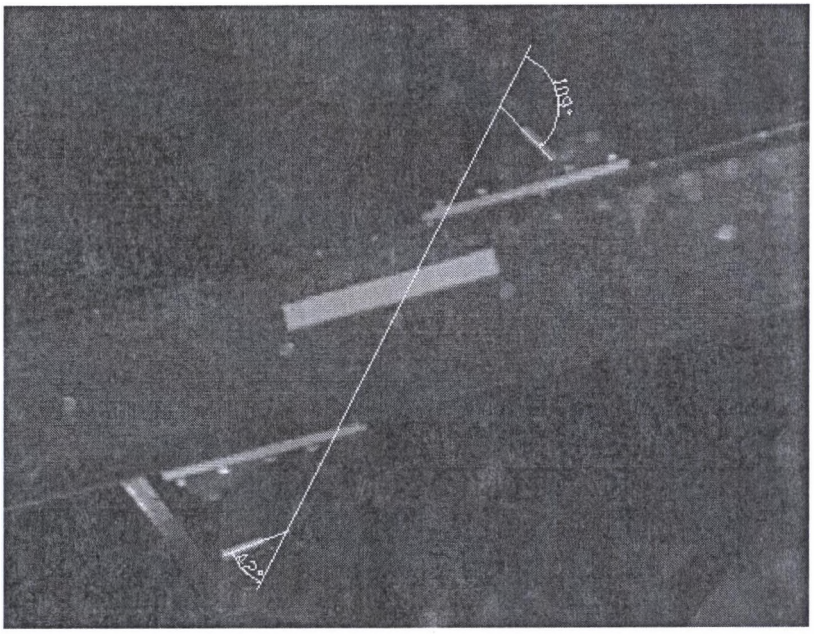

Synchronisation $\omega_1=\omega_2$

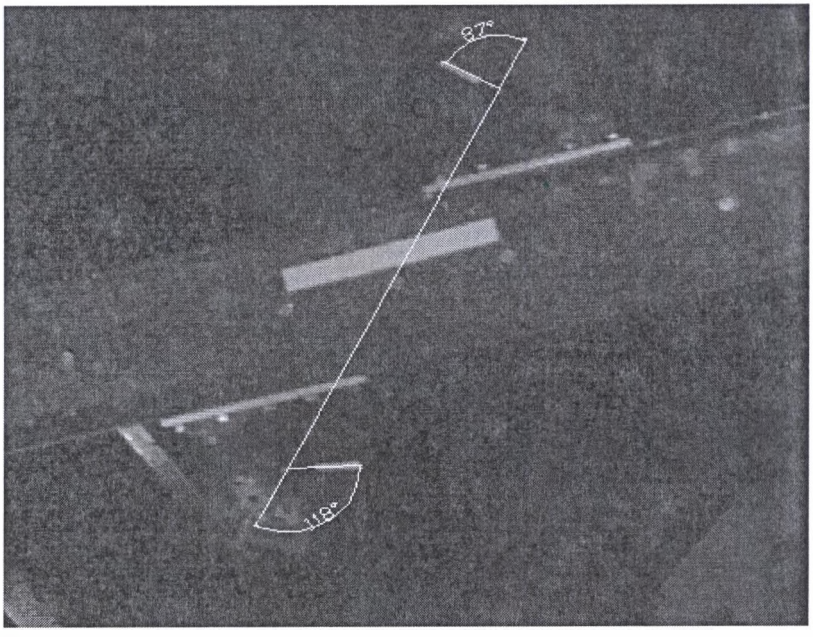

Fig. 9. Setting 2, F = 4,77 kN
Rys. 9. Ustawienie 2, F = 4,77 kN

Synchronisation $\omega_1=-\omega_2$

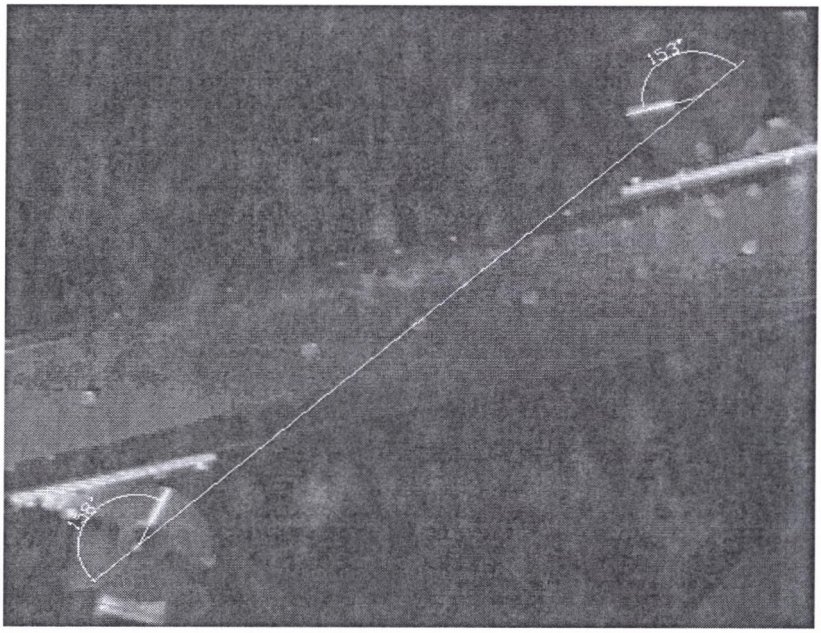

Synchronisation $\omega_1=\omega_2$

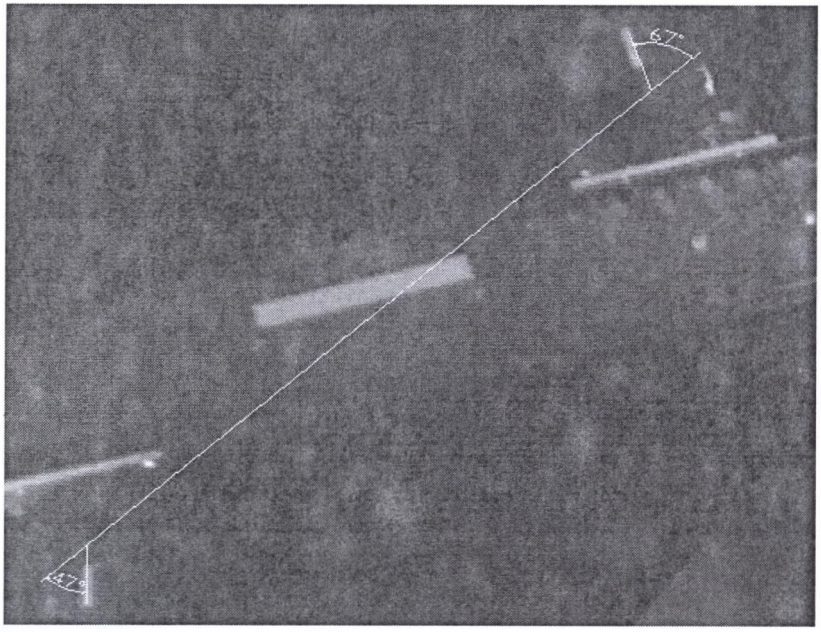

Fig. 10. Setting 3, F = 2 kN
Rys. 10. Ustawienie 3, F = 2 kN

- for maximum (F = 10 kN) and minimum value (F = 2kN) of the exciting force at counter-current synchronisation.

$$\lambda = \phi_2 - \phi_1$$

- for mean value (F = 4.77 kN) of the exciting force at counter-current synchronisation.

$$\lambda = |\phi_2 - 54°| - |\phi_1 - 54°|$$

- for maximum (F = 10 kN) and minimum value (F = 2kN) of the exciting force at cocurrent synchronisation.

$$\lambda = \phi_1 + (180° - \phi_2)$$

- for mean value (F = 4.77 kN) of the exciting force at cocurrent synchronisation.

$$\lambda = (\phi_1 + 54°) + [180° - (\phi_2 + 54°)]$$

Examples of the results of measurements are given in Table 2 (setting 2). The measured values of the phase shift angle λ for all tested configurations of the driving system are shown in Table 3.

Table 2

Results of measurements of the phase shift angle

SETTING 2 (s = 200 mm)						
EXCITING FORCE	DRIVE TYPE	No. of MEASU-REMENT	UPPER VIBRATOR ϕ_1 [°]	LOWER VIBRATOR ϕ_2 [°]	λ [°]	λ_{mean} [°]
1	2	3	4	5	6	7
F = 10 kN	COCURRENT SYNCHRONISATION $\omega_1=\omega_2$	0	5	5	180	176°10'
		1	11	17	174	
		2	21	24	177	
		3	32	33	179	
		4	37	44	173	
		5	51	57	174	
	COUNTER-CURRENT SYNCHRONISATION $\omega_1=-\omega_2$	0	114	121	7	10°50'
		1	112	130	11	
		2	121	140	7	
		3	133	148	12	
		4	143	157	8	
		5	153	167	10	
F = 4.77 kN	COCURRENT SYNCHRONISATION $\omega_1=\omega_2$	0	87	118	149	148°30'
		1	94	126	148	
		2	98	133	145	
		3	107	138	149	
		4	118	145	153	
		5	116	149	147	
	COUNTER-CURRENT SYNCHRONISATION	0	109	42	43	42°10'
		1	113	37	42	
		2	119	31	42	
		3	125	27	44	

	$\omega_1=-\omega_2$	4	130	20	42	
		5	135	13	40	
F = 2 kN	COCURRENT SYNCHRONISATION $\omega_1=\omega_2$	0	17	24	173	171°50'
		1	22	29	173	
		2	27	36	171	
		3	29	40	169	
		4	36	45	171	
		5	44	50	174	
	COUNTER-CURRENT SYNCHRONISATION $\omega_1=-\omega_2$	0	29	39	10	9°19'
		1	24	35	11	
		2	20	30	10	
		3	14	22	8	
		4	10	17	7	
		5	1	11	10	

Table 3

The angle of phase shift λ for all tested configurations of the drive system

Synch. $\omega_1=\omega_2$	Setting of vibrators		
exciting force	1 (s = 50mm)	2 (s = 200mm)	3 (s = 400mm)
minimum (F=2kN)	180°50'	171°50'	164°10'
mean (F=4.77 kN)	154°00'	148°30'	178°20'
maximum (F=10kN)	180°20'	176°10'	180°40'
Synch. $\omega_1=-\omega_2$	Setting of vibrators		
exciting force	1 (s = 50mm)	2 (s = 200mm)	3 (s = 400mm)
minimum (F=2kN)	25°50'	9°19'	24°10'
mean (F=4.77 kN)	3°30'	42°10'	15°49'
maximum (F=10kN)	9°10'	10°50'	9°10

Concluding remarks

Analysis of the phase shift angle λ showed that it remained constant after the conditions of screen operation stabilised (i.e. in several seconds) and depended only on the configuration of the screen driving system (during tests no differences occurred in the measurement of angle λ bigger than those resulting from the accuracy of measurement). This observation confirms the thesis that the self-synchronisation is a stable phenomenon.

When measuring the phase shift, for the cocurrent synchronisation in setting 1, for minimum and maximum values of the exciting force, the shift is equal to 180°, while for the mean exciting force it decreases to 154°. For setting 2, the phase shift is 170° and 180° for minimum and maximum exciting force, respectively, and decreases down to 148°30'for the mean force. The case is different for setting 3, where for minimum and maximum values of

the exciting force, the angle is 164°10' and 180°, while for the mean force it is 178°20'. The angle of phase shift is close to 180° which is the next evidence of torsional vibrations.

When analysing results for the counter-current synchronisation, it can be observed that for the three settings at a maximum exciting force the angle is around 10°, while for mean force this shift is 3°30', while for minimum value of the exciting force the angle is close to 25° in all cases.

The angle of phase shift affects the value of resultant exciting force generated by the vibrators, and consequently, the motion of the riddle itself. The change of parameters of the drive has a significant effect on the process of screening. Important for the riddle motion are torsional vibrations. It is known that the riddle motion consists of component motion along x and y axes and torsional motion around the centre of gravity. It is important that the riddle moves with slight torsional vibrations which contributes to intensive motion of the material on the sieve beginning and end (spread of the layer and additional screening). However, a too big contribution of torsional vibrations to the oscillating motion of the riddle, causes build-up of material in the middle of the sieve and makes the process of screening uncontrollable. This effect is a result of change in the character of the riddle motion which in turn changes the value of dynamic factor K and the angle of sieve trajectory β. Construction of a dynamic model of the screen that would be as close as possible to the results of measurements is very important for proposing a process model that will be used to select the most suitable configuration of the screen drive for a given material.

REFERENCES

1. Banaszewski T.: Przesiewacze. Wydawnictwo Śląsk, Katowice 1990.
2. Blechman I. I.: Sinchronizacje dinamiczeskich sistiem, Moskwa-Leningrad 1976.
3. Dietrych J.: Teoria i budowa przesiewaczy. WGH, Katowice 1962.
4. Sztaba K.: Przesiewanie. Śląskie Wydawnictwo Techniczne, Katowice 1993.
5. Wodziński P.: Odsiewanie materiałów ziarnistych; Rozprawy Naukowe z. 40 Zeszyty Naukowe PŁ.

Recenzent: Dr hab. inż. Aleksander Lutyński
Profesor Politechniki Śląskiej

Streszczenie

Przesiewacze krążące jednopłaszczyznowe charakteryzują się tym, że rzeszoto wykonuje ruch drgający w płaszczyźnie wzdłużnej maszyny, tzn. w płaszczyźnie prostopadłej do powierzchni sita i równoległej do ścian bocznych rzeszota, oraz do wypadkowego kierunku transportu materiału na sicie [1,2,3,4]. W chwili obecnej maszyny tego typu stanowią co najmniej 90% badanych i eksploatowanych maszyn przesiewających. Coraz częściej konstruktorzy tego typu maszyn wykorzystują zjawisko samosynchronizacji wibratorów napędowych. Pozwala to w znacznym stopniu uprościć konstrukcję układu napędowego przesiewacza, a co za tym idzie - zmniejszyć jego awaryjność i koszty obsługi.

W niniejszym opracowaniu przedstawiono wyniki badań przeprowadzonych na przesiewaczu liniowo-eliptycznym, jednej z konstrukcji, które powstały w Katedrze Aparatury Procesowej Wydziału Inżynierii Procesowej i Ochrony Środowiska Politechniki Łódzkiej [5]. Jest to nowoczesna maszyna, pozwalająca jednocześnie na wykorzystanie wszystkich znanych dotąd rozwiązań poszczególnych elementów składowych przesiewacza, np. zawieszeń, sit, mocowania sit itp.

Przesiewacz ten zbudowany jest z dwóch wibratorów napędowych oraz prostopadłościennego rzeszota zamontowanego na zawieszeniu sprężystym. Takie rozwiązanie umożliwia zmianę pochylenia rzeszota w zakresie od 0 - 20° oraz zmianę rozstawu wibratorów w zakresie od 0 mm do 800 mm. Przesiewacz ten jest maszyną o wymiarach sita B*L=300*1300 mm i całkowitej masie drgającej 180 kg. Do napędu przesiewacza używa się elektrowibratorów o prędkości znamionowej n =1400 min^{-1} z możliwością regulacji tej prędkości poprzez zmianę częstości prądu zasilającego. Dodatkowo istnieje możliwość regulacji siły wymuszającej wibratorów poprzez zmianę wzajemnego położenia mas niewyważonych. W badaniach używa się na ogół tylko jednej, nominalnej prędkości obrotowej. Układ napędowy pozwala zastosować dwie różne konfiguracje napędowe: współbieżną i przeciwbieżną. W pracy filmowano ruch mas niewyważonych, napędzających przesiewacz i ich wzajemne położenie w trakcie tegoż ruchu. Określono tory sit (teoretyczne i rzeczywiste) oraz kąt przesunięcia fazowego tych mas.